JPET Fast Forward. Published on November 2, 2023 as DOI: 10.1124/jpet.123.001772
This article has not been copyedited and formatted. The final version may differ from this version.

High dose acetaminophen with concurrent CYP2E1 inhibition has profound anti-cancer activity without liver toxicity

Allyn Bryan, Pavani Pingali, Anthony Faber, Joseph Landry, Jephte Y. Akakpo, Hartmut Jaeschke, Howard Li, Won Lee, Lauren May, Bhaumik Patel, Alex Neuwelt

AB, PP, WL, BP, AN: Department of Veterans Affairs, Richmond, Virginia.

TF: Department of Oral and Craniofacial Molecular Biology, Virginia Commonwealth University

JL, LM: Department of Human and Molecular Genetics, Virginia Commonwealth University

HL: Department of Veterans Affairs, Charleston, SC.

HJ, JA: Department of Pharmacology, Toxicology & Therapeutics, University of Kansas

JPET Fast Forward. Published on November 2, 2023 as DOI: 10.1124/jpet.123.001772
This article has not been copyedited and formatted. The final version may differ from this version.

High dose acetaminophen with concurrent CYP2E1 inhibition

Corresponding Author:

Alexander Neuwelt, MD.

1201 Broad Rock Blvd

Richmond, Va

23249

Alexander.neuwelt@va.gov

Ph: 804-675-5446

F: 804-675-5447

Number of pages: 23

# of Figures: 6

# of References: 38

# of words in Abstract: 196

# of words in Introduction: 524

# of words in Discussion: 776

Abbreviations:

AAP: Acetaminophen

AM404: N-acylphenolamine

NAC: N-acetylcysteine

NAPQI: N-acetyl-p-benzoquinone imine

Recommended section assignment: Toxicology

JPET Fast Forward. Published on November 2, 2023 as DOI: 10.1124/jpet.123.001772
This article has not been copyedited and formatted. The final version may differ from this version.

Abstract

Acetaminophen (AAP) is metabolized by a variety of pathways such as sulfation, glucuronidation and fatty acid amide hydrolase-mediated conversion to the active analgesic metabolite AM404. CYP2E1-mediated metabolism to the hepatotoxic reactive metabolite NAPQI (N-acetyl-p-benzoquinone imine) is a minor metabolic pathway that has not been clearly linked to AAP therapeutic benefits yet definitely leads to AAP liver toxicity. N-acetylcysteine (NAC) (an antioxidant) and fomepizole (a CYP2E1 inhibitor) are clinically used for the treatment of AAP toxicity. Mice treated with AAP in combination with fomepizole (+/- NAC) were assessed for liver toxicity by histology and serum chemistry. Anti-cancer activity of AAP with NAC and fomepizole rescue was assessed in vitro and in vivo. Fomepizole with or without NAC completely prevented AAP-induced liver toxicity. In vivo, high dose AAP with NAC/fomepizole rescue had profound anti-tumor activity against commonly used 4T1 breast tumor and LLC lung tumor models and no liver toxicity was detected. The anti-tumor efficacy was reduced in immune-compromised NSG mice, suggesting an immune mediated mechanism of action. In conclusion, using fomepizole-based rescue, we were able to treat mice with 100-fold higher than standard dosing of AAP (650 mg/kg) without any detected liver toxicity and substantial anti-tumor activity.

JPET Fast Forward. Published on November 2, 2023 as DOI: 10.1124/jpet.123.001772
This article has not been copyedited and formatted. The final version may differ from this version.

Significance Statement

High dose acetaminophen (AAP) can be given concurrently with CYP2E1 inhibition to allow for safe dose escalation to levels needed for anti-cancer activity without detected evidence of toxicity.

JPET Fast Forward. Published on November 2, 2023 as DOI: 10.1124/jpet.123.001772
This article has not been copyedited and formatted. The final version may differ from this version.

Introduction

Acetaminophen (AAP) is metabolized by a variety of pathways including glucuronidation, sulfation, and fatty acid amide hydrolase (FAAH) mediated conversion to the active analgesic metabolite N-acylphenolamine (AM404) (Ohashi and Kohno, 2020). Additionally, CYP2E1-mediated conversion of AAP into a transient reactive intermediate, NAPQI (N-acetyl-p-benzoquinone imine) is a minor metabolic pathway, comprising 10% of AAP metabolism. Within the liver, NAPQI is rapidly detoxified by glutathione (GSH) and in overdose hepatic GSH becomes depleted leading to free-radical mediated liver toxicity (Heard, 2008).

The CYP2E1 metabolic pathway is clearly responsible for the toxicity of AAP; CYP2E1 KO mice are essentially immune from high dose AAP-induced liver damage (Lee et al., 1996). However, considering NAPQI is a transient reactive intermediate byproduct of a minor metabolic pathway that is rapidly detoxified by GSH in the liver, it is unlikely that CYP2E1 metabolism is required for AAP therapeutic efficacy. In fact, we have demonstrated in multiple models that glutathione depletion selectively occurs in the liver and not the tumor (Pingali et al., 2021; Wu et al., 2013); the selective glutathione depletion within the liver is likely secondary to increased CYP2E1 expression in hepatocytes relative to other organs (Bieche et al., 2007). Despite observing no glutathione depletion in the tumor, we have consistently observed anti-cancer efficacy of high dose AAP suggesting a CYP2E1 independent mechanism of action (Neuwelt et al., 2014; Neuwelt et al., 2009).

High dose AAP has demonstrated promising results for the treatment of cancer both pre-clinically and clinically. In a phase I clinical trial of high dose AAP using N-acetylcysteine (NAC) rescue, the response rate was 20% among assessable patients without achieving dose limiting toxicity (Kobrinsky et al., 1996). Drugs with at least a 20% response rate in phase I (fewer than 10% of drugs tested) meet primary endpoints in subsequent phase II trials 51% of the time (Bugano et al., 2017). Despite demonstrating promise in phase I, AAP has not been studied in

JPET Fast Forward. Published on November 2, 2023 as DOI: 10.1124/jpet.123.001772
This article has not been copyedited and formatted. The final version may differ from this version.

subsequent phase trials. The lack of further clinical evaluation is in part attributable to lack of mechanistic understanding.

NAC is the FDA-approved antidote for AAP toxicity. However, there is no large human randomized studies demonstrating the efficacy of NAC; the efficacy is mostly based on case series-level data. A Cochrane report acknowledges the limited evidence for NAC monotherapy (Brok et al., 2006). There are multiple clinical case reports of combination rescue strategies involving fomepizole and NAC with or without dialysis for the management of massive AAP overdose (Chiu et al., 2021; Pourbagher-Shahri et al., 2022). Fomepizole is generally safe and widely available considering it is FDA-approved for methanol and ethylene glycol toxicity (Rasamison et al., 2020). Fomepizole is a potent CYP2E1 inhibitor (Hazai et al., 2002), thus preventing AAP-induced NAPQI formation and resultant hepatotoxicity (Akakpo et al., 2018). Additionally, fomepizole inhibits c-jun N-terminal kinase (JNK) thus decreasing free-radical mediated stress signaling in the mitochondria (Akakpo et al., 2019). As a result, fomepizole is increasingly being used as an adjunctive therapy for massive AAP poisoning in the clinic (Filip et al., 2022).

In the present manuscript we evaluate the novel approach of using fomepizole concurrently with high dose AAP for enhanced therapeutic benefits while preventing hepatotoxicity.

JPET Fast Forward. Published on November 2, 2023 as DOI: 10.1124/jpet.123.001772
This article has not been copyedited and formatted. The final version may differ from this version.

Materials and Methods

Cell lines. LLC-Luc cells were obtained from ATCC. 4T1 and MDA-MB-231 cells were obtained from collaborator Joseph Landry (Department of Genetics, VCU). Cell lines were routinely validated using morphology and were checked for mycoplasma using a commercial kit (ATCC). Authenticity of lines was confirmed using short-tandem repeat analysis.

Mouse studies. 8-12 week old BALB/c mice and C57bl/6 mice were obtained from Jackson labs. NSG mice were obtained from VCU Cancer Mouse Modeling Core facility. All studies were conducted with approval of our institutional IACUC committee (Protocol 02444). ALT (alanine transaminase) and BUN (blood urea nitrogen) were measured in the clinical lab at the Richmond VA Medical Center. Liver H&E slides were prepared at the VCU Tissue and Data Acquisition Analysis Core facility and analyzed by pathologist Won Lee. Fomepizole was obtained from Selleck and diluted in PBS as appropriate. Acetaminophen (AAP) was obtained from Sigma and diluted in 10% glucose in warmed water prior to injection. NAC was obtained from Sigma and dissolved in 10% glucose in water. For 2′,7′-Dichlorofluorescein diacetate (DCFH-DA) assays, 4T1 tumor bearing mice were treated as indicated. Frozen sections were obtained of tumors, and slides containing 5 micrometer thick tissue slices were incubated for 30 min with 5 μM DCFH-DA dye prior to imaging with a Zeiss LSM 700 confocal microscope (488 laser). The optical magnification was 40x (oil objective). At time of animal sacrifice serum was taken and used to measure LDH levels using Cyquant assay (Fisher), n=3 replicates per condition. Portions of the tumor were homogenized into a protein lysate. Glutathione levels (reduced and total) were measured using the Glutathione Colorimetric Assay Kit (Fisher) and normalized for total protein levels, n=3 replicates per condition. Experiment repeated in two different tumor models, LLC and 4T1. Data graphed using Graphpad Prism software.

Orthotopic lung tumor models. *Intratracheal model*: LLC-luc cells (100,000) were injected intra-tracheally in 20% matrigel via intra-tracheal intubation. Tumor growth was monitored using IVIS Spectrum In Vivo Imaging System (PerkinElmer) after injection of D-luciferin (Gold Bio) IP.

JPET Fast Forward. Published on November 2, 2023 as DOI: 10.1124/jpet.123.001772
This article has not been copyedited and formatted. The final version may differ from this version.

IVIS quantification performed using internal PerkinElmer system software for evaluation of region of interest. *Surgical model*: 100,000 LLC-luc cells were implanted orthopically into the left lobe of male C57bl/6 mice using previously published protocols (Kwak et al., 2018). Treatment was 2x/week starting about 5 days after inoculation (eg when visible signal appeared on IVIS imaging). Mice were sacrificed on about day 21. Tumor measurements were made after animal sacrifice using equation ½ (Length x Width^2). Number of replicates (mice) shown in respected Figure Legends.

Orthotopic breast tumor models. 4T1 tumors were inoculated via direct injection in the breast tissue (mammary fat pad) of female BALB/c mice. Once tumors became palpable, treatment was initiated. Treatment was IP 2x/week. Tumor size was measured at least 2x/wk using digital calipers and tumor size calculated using formula ½ (Length x Width^2). The vehicle for both AAP and rescue cocktails (NAC, fomepizole) was 10% glucose in warmed water. When indicated, propylene glycol 10% was also included in the vehicle.

Acetaminophen levels. ELISA was used to evaluate acetaminophen levels using a kit from Immunalysis (ref 227-0096). N=2 replicates per condition.

Viability and cytotoxicity assays. Cells were treated as indicated. After 48 hours, viability was assessed using CCK8 assay per manufacturer's protocol (Dojindo). Experiment was performed in triplicate. Experiment was performed one time each in 3 separate cell lines (LLC, 4T1, MDA-MB-231). Additionally, the conditioned medium was assess for lactate dehydrogenase (LDH) levels using the Cyquant assay (Thermo Fisher). Experiment performed in triplicate one time each in 2 separate cell lines (LLC and 4T1). Data was processed and graphed using Graphpad Prism software.

qPCR. RNA quantification was performed using our previously published methodologies(Pingali et al., 2021). Primers used are CYP2E1 mouse forward TTCAGCGGTTCATCACCCT and reverse GAGGTATCCTCTGAAAATGGTGTC. GAPDH mouse forward CATGGCCTTCCGTGTTCCTA

JPET Fast Forward. Published on November 2, 2023 as DOI: 10.1124/jpet.123.001772
This article has not been copyedited and formatted. The final version may differ from this version.

and reverse TGTCATCATACTTGGCAGGTTTCT. Data performed in triplicate.

JC-1 assay of mitochondrial membrane potential. Mouse hepatocytes were obtained from collaborator Huiping Zhou using published protocols (Zhou et al., 2006). Hepatocytes were treated as indicated and incubated with JC-1 dye (Biotium) per manufacturers protocol. Microscopy was performed at the VCU microscopy core facility using a Zeiss LSM 700 confocal microscope. The optical magnification was 40x (oil objective). Live-cell imaging was performed using the 488 laser to image green and 555 laser to image red.

Study approval. All studies were conducted with approval of our institutional IACUC committee (Protocol 02444).

Protein adduct measurement. Snap frozen liver and tumor tissues were homogenized in 10 mM sodium acetate (pH 6.5) using a blade-type homogenizer. Supernatants were collected after centrifugation of the homogenate at 16,000 g for 5 minutes. To remove low molecular weight compounds which might interfere with the measurement, the supernatants were filtered through Bio-Spin 6 columns (Bio-Rad, Hercules, CA), which were pre-washed with 10 mM sodium acetate. The filtrates were subjected to overnight protease digestion to separate the APAP-Cys adducts from proteins which were then precipitated using ice cold 40% trichloroacetic acid (Sigma Aldrich, St. Louis, Missouri). The supernatant was collected and filtered through microcentrifuge tubes. APAP-CYS was then measured using HPLC with electrochemical detection as described (Akakpo et al., 2018).

Statistical analysis. All data are presented as mean ± S.D. The student-T test was used for the comparison of measurable variants between 2 groups. Two-way ANOVA with Bonferroni post-test was used for statistical comparisons between groups in tumor growth. $P \leq 0.05$ was considered statistically significant. Grubbs outlier test was used to exclude extreme outliers (only Figure 5 mouse 4 day 16 and mouse 5 day 24) for BLI statistics. Note that this exclusion does not affect biological interpretation of data—outliers were in the same direction as overall

JPET Fast Forward. Published on November 2, 2023 as DOI: 10.1124/jpet.123.001772
This article has not been copyedited and formatted. The final version may differ from this version.

trend (GraphPad Prism 6.0; Graph Pad Software). Data processing and graphing was performed using GraphPad Prism Software.

Data availability. All primary data is available upon request.

Results

Efficacy of clinically used AAP antidotes for preventing hepatotoxicity. In the clinic, fomepizole and NAC are used to treat AAP poisoning—though only NAC is FDA approved for this purpose (Filip et al., 2022; Heard, 2008). We thus sought to evaluate the efficacy of fomepizole and NAC in preventing AAP toxicity in our mouse models. BALB/c mice were treated with AAP alone and in combination with fomepizole +/- NAC. The following day, the mice were weighed and sacrificed. Serum was collected for analysis and liver histology assessed. Fomepizole prevented AAP hepatotoxicity, as assessed by serum ALT levels and liver morphology (per review by pathologist WL), but NAC did not. Additionally, the combination of NAC + fomepizole was also an effective cocktail for preventing AAP liver injury and weight loss (Figure 1 A-D). In fact, there was no significant difference between ALT values in untreated mice (average ALT 28 +/- 4) versus those treated with 650 mg/kg AAP concurrently with fomepizole/NAC rescue (average ALT 46 +/- 18, $p = 0.16$). ELISA was used to measure AAP levels at the doses used: At 1 hour post-treatment of 650 mg/kg AAP, levels were 399 µg/mL and decreased to 298 µg/mL at 2 hours post-treatment (Figure 1E). These serum levels are comparable to what was achieved in a clinical trial of high dose oral AAP with delayed NAC rescue (mean serum concentration 245 ug/mL, range 95-473 ug/mL) (Kobrinsky et al., 1996).

NAC/fomepizole rescue does not compromise anti-cancer activity of high dose AAP in vitro. The Protein Atlas was used to evaluate expression of CYP2E1 in various organs. It was demonstrated that CYP2E1 is expressed in the liver and no other organ (Figure 2A) (note: CYP2E1 levels have been determined in mouse and human kidneys in other studies (Akakpo et al., 2020)). Because CYP2E1 mediates conversion of AAP into a toxic reactive metabolite that

JPET Fast Forward. Published on November 2, 2023 as DOI: 10.1124/jpet.123.001772
This article has not been copyedited and formatted. The final version may differ from this version.

can be neutralized by antioxidants such as NAC, we evaluated whether a rescue regimen comprised of the CYP2E1 inhibitor fomepizole and NAC reverses anti-tumor activity of high dose AAP. We demonstrate in 4T1 and MDA-MB-231 breast cancer cells in addition to LLC-luc lung cancer cells that NAC/fomepizole rescue does not reverse AAP cytotoxicity in vitro (Figure 2 B-D, Supplemental Figure 1). In 4T1 tumor bearing mice, CYP2E1 was expressed at high levels in the liver, but not the tumor (Figure 2E), potentially explaining the differential effects of NAC/fomepizole rescue on the tumor and liver.

We have previously shown that AAP selectively depletes glutathione in the liver but not the tumor in multiple xenograft models (Pingali et al., 2021; Wu et al., 2013). Extensive prior research demonstrates that NAC helps prevent AAP-induced reactive metabolite-mediated injury and resultant glutathione depletion ultimately leading to mitochondrial injury in the liver (Saito et al., 2010). We next sought to determine if fomepizole has similar benefits. Hepatocytes isolated from a mouse liver were treated for 6 hours with or without fomepizole rescue and analyzed with JC-1 dye (a sensitive marker for mitochondrial membrane potential) using confocal microscopy. We demonstrate that AAP led to mitochondrial depolarization (decrease in red/green ratio) that was reversed by fomepizole (Figure 3A). In vivo, 4T1 tumor bearing mice were treated with AAP with or without fomepizole and 6 hours later the tumor and liver were assessed for free radical levels using DCFH dye (a sensitive indicator for reactive oxygen species in cells). AAP created high levels of free radicals in the liver but not the tumor, and fomepizole effectively rescued the free radical injury in the livers of AAP-treated mice (Figure 3B). Plasma levels of LDH, which can be used as a marker of hepatotoxicity (Kotoh et al., 2011), were elevated in the AAP-treated mice and corrected with concurrent fomepizole rescue (Figure 3C).

Protein adducts are formed by hepatic metabolism of acetaminophen to the reactive intermediate NAPQI, which covalently binds to hepatic proteins (James et al., 2009). AAP treatment led to a large accumulation of protein adducts in the liver but not the tumor.

JPET Fast Forward. Published on November 2, 2023 as DOI: 10.1124/jpet.123.001772
This article has not been copyedited and formatted. The final version may differ from this version.

Fomepizole effectively prevented AAP-induced hepatic protein adduct formation (Figure 3D). Similarly, high dose AAP depleted the levels of GSH in the liver consistent with the known conjugation of NAPQI. AAP-induced GSH depletion was reversed by fomepizole. On the other hand, no changes in GSH levels were observed in the tumor upon treatment with AAP (Figure 3 E; Supplemental Figure 2). AAP concentrations were similar in the tumor and liver suggesting that distinct patterns of drug distribution do not account for the observed changes in GSH depletion and protein adduct formation (Supplemental Figure 3).

High dose AAP has anti-tumor activity in vivo without liver toxicity. We next sought to evaluate the efficacy of high dose AAP with NAC/fomepizole rescue in treating orthotopic 4T1 tumors. (Note, while NAC may not be necessary for rescue in our mouse models—see Figure 1—we nevertheless used a NAC/fomepizole rescue regimen given the established role of NAC in treating clinical AAP toxicity). Our results demonstrated an approximately 50% decrease in tumor growth in 4T1 tumors treated with 650 mg/kg AAP and NAC/fomepizole rescue relative to NAC/fomepizole alone (Figure 4A). The mice treated high dose AAP had no weight loss and in fact gained weight during the course of the study (Figure 4A). NAC/fomepizole alone did not modulate tumor growth relative to untreated mice (Supplemental Figure 4).

To determine if other CYP2E1 inhibitors besides fomepizole may be used to mitigate AAP toxicity while preserving anti-tumor efficacy, we performed a similar experiment using NAC/propylene glycol (PG) rescue. PG is known to be a CYP2E1 inhibitor that helps prevent AAP toxicity (Thomsen et al., 1995). The in vivo anti-tumor activity of high dose AAP was virtually identical using PG/NAC rescue relative to fomepizole/NAC rescue (Figure 4B). However, mice treated with high dose AAP with PG/NAC rescue did lose weight (6% on average) while mice treated with PG/NAC alone gained weight (7% on average). Importantly, neither regimen was associated with liver toxicity as determined by serum ALT and liver histology (Figure 4C, D). A small increase in BUN was observed in the mice treated with AAP

JPET Fast Forward. Published on November 2, 2023 as DOI: 10.1124/jpet.123.001772
This article has not been copyedited and formatted. The final version may differ from this version.

with PG/NAC rescue, but no increase in BUN was observed following NAC/fomepizole rescue (Figure 4C, Supplemental Figure 5).

We next evaluated the anti-tumor efficacy of high dose AAP using an orthotopic syngeneic model of lung cancer. LLC-luc cells were injected intra-tracheally into C57bl/6 mice and treated twice weekly with 650 mg/kg AAP with NAC/fomepizole versus rescue alone. It was demonstrated that AAP treated mice had markedly reduced tumor burden relative to control mice (Figure 5A). At the conclusion of the experiment, lung weights were lower in AAP-treated mice likely reflecting lower tumor burden. Additionally, over the course of the experiment, mice treated with AAP gained weight while control mice lost weight, likely a result of differences in tumor burden (Figure 5 B, C, Supplemental Figure 6). Confirming the IVIS results, histologic evaluation revealed tumor in 0/9 evaluated sections in mouse 9 treated with AAP/NAC/fomepizole and 9/9 sections in mouse 5 treated with NAC/fomepizole alone (Figure 5D). A representative section (Figure 5E) reveals tumor infiltrated lung in the vehicle-treated mouse and normal lung in the AAP-treated mouse.

Using a surgical orthotopic technique, LLC-luc cells were implanted into the left lobe of C57bl/6 mice. Mice were treated with AAP and NAC/PG rescue versus NAC/PG alone. AAP again had profound anti-tumor activity in this model (Figure 6 A-C, Supplemental Figure 7). Only mice in the vehicle arm lost weight, likely a result of increased tumor burden in mice not receiving AAP (Figure 6D). We then repeated the experiment using immune-compromised NSG mice. Interestingly, there was no anti-tumor activity of AAP in these mice (Figure 6E, F). These data altogether demonstrate that AAP exerts an immune-mediated mechanism of anti-cancer activity.

JPET Fast Forward. Published on November 2, 2023 as DOI: 10.1124/jpet.123.001772
This article has not been copyedited and formatted. The final version may differ from this version.

Discussion

CYP2E1-mediated metabolism has not been definitively linked to AAP therapeutic benefits such as analgesia and anti-tumor activity. In the present study, we demonstrate that concurrent administration with CYP2E1 inhibition with fomepizole allows for dose escalation to 100-fold higher than standard AAP dosing (650 mg/kg, or about 50 grams in average 75 kg human adult) without any detectable liver toxicity (Figure 1) and without compromising anti-tumor activity (Figure 2). Further, high dose AAP with fomepizole/NAC rescue has profound anti-tumor activity against commonly used syngeneic orthotopic models of breast cancer (4T1) and lung cancer (LLC-luc) (Figures 4-6). Mouse syngeneic tumor models (4T1 and LLC) were used for in vivo studies because AAP appears to lose activity in immune-compromised animals (NSG mice, see Figure 6) used to grow human tumors. Both 4T1 and LLC are known to be resistant to standard first line therapies including PD-1 (Kim et al., 2014; Li et al., 2017), and cisplatin (Merritt et al., 2003) (Note: PD-1 clinically is used first line in both lung and breast cancer; cisplatin is first line in lung cancer but not breast cancer).

The mechanism of anti-cancer activity of high dose AAP has not been definitively characterized. We have previously shown that AAP has anti-cancer stem cell activity via a STAT3-dependent mechanism. Additionally, AAP directly binds to STAT3 and has a high degree of specificity for STAT3 relative to STAT1 (Pingali et al., 2021).

In addition to direct effects on the tumor cell (eg via STAT3 inhibition), AAP may also modulate JAK-STAT signaling in the tumor immune micro-environment. In the innate immune system, STAT1 signaling mediates conversion of macrophages to an activated anti-tumor “M1 phenotype” whereas STAT3 and STAT6 are more closely associated with immune-suppressive “M2” tumor associated macrophages (Xiao et al., 2020). Similarly, the various JAK-STAT signaling pathways modulate differentiation of T-cells towards a cytotoxic versus regulatory phenotype (Villarino et al., 2015). Our data suggests that AAP has a substantially reduced efficacy in NSG mice with defective innate and adaptive immune systems, arguing that AAP

JPET Fast Forward. Published on November 2, 2023 as DOI: 10.1124/jpet.123.001772
This article has not been copyedited and formatted. The final version may differ from this version.

may function at least in part via modulation of the anti-tumor immune response (Figure 6). While at standard doses AAP is not felt to have anti-inflammatory or immune modulatory properties, at high doses the effects of AAP on systemic inflammation have not been studied. The effect of AAP on the anti-tumor immune response (particularly tumor associated macrophage polarization/activation) is of great interest and the subject of ongoing studies within our laboratory (Bryan, 2023).

Administering rescue agents to allow for dose escalation of anti-cancer therapeutics is an established approach. For instance, leucovorin is a folic acid derivative that allows for synthesis of nucleic acids even in the presence of high doses of methotrexate, thus mitigating methotrexate toxicities such as myelosuppression and gastrointestinal toxicity. Concurrent administration of methotrexate and leucovorin has been widely adopted, particularly in the setting of malignant lymphomas (Flombaum and Meyers, 1999). Concurrent administration of CYP2E1 inhibitors and AAP may have analogous benefits for the treatment of patients with advanced malignancies such as breast and lung cancer.

The relative lack of efficacy of NAC for preventing hepatotoxicity in our models is unexpected given the established role of NAC as an antidote to AAP toxicity (Akakpo et al., 2022; Heard, 2008). Prior pre-clinical studies of NAC yielded mixed results in preventing AAP liver toxicity (Khayyat et al., 2016; Saito et al., 2010; Wang et al., 2021). Khayyat et al showed that NAC (106 mg/kg IP) administered 1.5 hours after AAP (400 mg/kg IP) decreased ALT from 940 (no NAC) to 860 U/L (+ NAC) relative to baseline ALT of 10 U/L (Khayyat et al., 2016). Wang et al demonstrated no protection (eg reversal of ALT elevation) of 100 mg/kg NAC IV 30 minutes after AAP (350 mg/kg IP) in C57BL/6 mice (Wang et al., 2021). Additional in vitro evidence suggests that physiologically relevant concentrations of NAC have minimal protective effect against CYP2E1-mediated AAP toxicity (Dai and Cederbaum, 1995). Nevertheless, there is a large body of literature supporting the use of NAC both pre-clinically (James et al., 2003; Owumi et al., 2015) and clinically (Heard, 2008). While there is conflicting pre-clinical data (an

JPET Fast Forward. Published on November 2, 2023 as DOI: 10.1124/jpet.123.001772
This article has not been copyedited and formatted. The final version may differ from this version.

effect that is likely model dependent), in the clinic NAC continues to have a well-established role in the treatment of AAP poisoning.

In the present work, we observe complete prevention of liver toxicity from AAP using concurrent fomepizole (Figure 1), a finding consistent with prior observations (Akakpo et al., 2022; Akakpo et al., 2019; Akakpo et al., 2018).

In conclusion, concurrent CYP2E1 inhibition is a novel approach that allows for safe dose escalation of AAP to levels that have profound anti-tumor activity in well-established pre-clinical lung and breast cancer models.

Acknowledgements

Authors appreciate assistance of Martha Joslyn, Rujul Kaul and Shellie Galabow for technical assistance.

All data available upon request. This article contains no datasets generated or analyzed during the current study.

Authors Contributions

Participated in research design: Bryan A, Neuwelt A, Faber A, Li H, Landry J, Patel B, May L, Jaeschke H

Conducted experiments: Bryan A, Neuwelt A, Pingali P, Akakpo J

Contributed new reagents or analytic tools: Lee W

Performed data analysis: Bryan A, Neuwelt A

Wrote or contributed to the writing of the manuscript: Neuwelt, A

References

Akakpo JY, Ramachandran A, Curry SC, Rumack BH and Jaeschke H (2022) Comparing N-acetylcysteine and 4-methylpyrazole as antidotes for acetaminophen overdose. *Arch Toxicol* 96:453-465.

Akakpo JY, Ramachandran A, Duan L, Schaich MA, Jaeschke MW, Freudenthal BD, Ding WX, Rumack BH and Jaeschke H (2019) Delayed Treatment With 4-Methylpyrazole Protects Against Acetaminophen Hepatotoxicity in Mice by Inhibition of c-Jun n-Terminal Kinase. *Toxicol Sci* 170:57-68.

Akakpo JY, Ramachandran A, Kandel SE, Ni HM, Kumer SC, Rumack BH and Jaeschke H (2018) 4-Methylpyrazole protects against acetaminophen hepatotoxicity in mice and in primary human hepatocytes. *Hum Exp Toxicol* 37:1310-1322.

Akakpo JY, Ramachandran A, Orhan H, Curry SC, Rumack BH, Jaeschke H (2020) 4-methylpyrazole protects against acetaminophen-induced acute kidney injury. Toxicol Appl Pharmacol. 2020 Dec 15;409:115317

Bieche I, Narjoz C, Asselah T, Vacher S, Marcellin P, Lidereau R, Beaune P and de Waziers I (2007) Reverse transcriptase-PCR quantification of mRNA levels from cytochrome (CYP)1, CYP2 and CYP3 families in 22 different human tissues. *Pharmacogenet Genomics* 17:731-742.

Brok J, Buckley N and Gluud C (2006) Interventions for paracetamol (acetaminophen) overdose. *Cochrane Database Syst Rev*:CD003328.

Bryan AL, Howard; Pingali, Pavani; Patel, Bhaumik; Neuwelt, Alexander (2023) High dose acetaminophen inhibits M2 polarization of tumor associated macrophages, in *AACR*, Orlando.

Bugano DDG, Hess K, Jardim DLF, Zer A, Meric-Bernstam F, Siu LL, Razak ARA and Hong DS (2017) Use of Expansion Cohorts in Phase I Trials and Probability of Success in Phase II for 381 Anticancer Drugs. *Clin Cancer Res* 23:4020-4026.

Chiu MH, Jaworska N, Li NL and Yarema M (2021) Massive Acetaminophen Overdose Treated Successfully with N-Acetylcysteine, Fomepizole, and Hemodialysis. *Case Rep Crit Care* 2021:6695967.

Dai Y and Cederbaum AI (1995) Cytotoxicity of acetaminophen in human cytochrome P4502E1-transfected HepG2 cells. *J Pharmacol Exp Ther* 273:1497-1505.

Filip AB, Berg SE, Mullins ME, Schwarz ES and Toxicology Investigators C (2022) Fomepizole as an adjunctive therapy for acetaminophen poisoning: cases reported to the toxicology investigators consortium (ToxIC) database 2015-2020. *Clin Toxicol (Phila)* 60:1006-1011.

Flombaum CD and Meyers PA (1999) High-dose leucovorin as sole therapy for methotrexate toxicity. *J Clin Oncol* 17:1589-1594.

Hazai E, Vereczkey L, Monostory K (2002) Reduction of toxic metabolite formation of acetaminophen. *Biochem Biophys Res Commun* 291:1089-1094.

Heard KJ (2008) Acetylcysteine for acetaminophen poisoning. *N Engl J Med* 359:285-292.

James LP, Letzig L, Simpson PM, Capparelli E, Roberts DW, Hinson JA, Davern TJ and Lee WM (2009) Pharmacokinetics of acetaminophen-protein adducts in adults with acetaminophen overdose and acute liver failure. *Drug Metab Dispos* 37:1779-1784.

James LP, McCullough SS, Lamps LW and Hinson JA (2003) Effect of N-acetylcysteine on acetaminophen toxicity in mice: relationship to reactive nitrogen and cytokine formation. *Toxicol Sci* 75:458-467.

Khayyat A, Tobwala S, Hart M and Ercal N (2016) N-acetylcysteine amide, a promising antidote for acetaminophen toxicity. *Toxicol Lett* 241:133-142.

Kim K, Skora AD, Li Z, Liu Q, Tam AJ, Blosser RL, Diaz LA, Jr., Papadopoulos N, Kinzler KW, Vogelstein B and Zhou S (2014) Eradication of metastatic mouse cancers resistant to immune checkpoint blockade by suppression of myeloid-derived cells. *Proc Natl Acad Sci U S A* 111:11774-11779.

Kobrinsky NL, Hartfield D, Horner H, Maksymiuk A, Minuk GY, White DF and Feldstein TJ (1996) Treatment of advanced malignancies with high-dose acetaminophen and N-acetylcysteine rescue. *Cancer Invest* 14:202-210.

Kotoh K, Kato M, Kohjima M, Tanaka M, Miyazaki M, Nakamura K, Enjoji M, Nakamuta M and Takayanagi R (2011) Lactate dehydrogenase production in hepatocytes is increased at an early stage of acute liver failure. *Exp Ther Med* 2:195-199.

Kwak JW, Laskowski J, Li HY, McSharry MV, Sippel TR, Bullock BL, Johnson AM, Poczobutt JM, Neuwelt AJ, Malkoski SP, Weiser-Evans MC, Lambris JD, Clambey ET, Thurman JM and Nemenoff RA (2018) Complement Activation via a C3a Receptor Pathway Alters CD4(+) T Lymphocytes and Mediates Lung Cancer Progression. *Cancer Res* 78:143-156.

Lee SS, Buters JT, Pineau T, Fernandez-Salguero P and Gonzalez FJ (1996) Role of CYP2E1 in the hepatotoxicity of acetaminophen. *J Biol Chem* 271:12063-12067.

Li HY, McSharry M, Bullock B, Nguyen TT, Kwak J, Poczobutt JM, Sippel TR, Heasley LE, Weiser-Evans MC, Clambey ET and Nemenoff RA (2017) The Tumor Microenvironment Regulates Sensitivity of Murine Lung Tumors to PD-1/PD-L1 Antibody Blockade. *Cancer Immunol Res* 5:767-777.

Merritt RE, Mahtabifard A, Yamada RE, Crystal RG and Korst RJ (2003) Cisplatin augments cytotoxic T-lymphocyte-mediated antitumor immunity in poorly immunogenic murine lung cancer. *J Thorac Cardiovasc Surg* 126:1609-1617.

Neuwelt AJ, Nguyen T, Wu YJ, Donson AM, Vibhakar R, Venkatamaran S, Amani V, Neuwelt EA, Rapkin LB and Foreman NK (2014) Preclinical high-dose acetaminophen with N-acetylcysteine rescue enhances the efficacy of cisplatin chemotherapy in atypical teratoid rhabdoid tumors. *Pediatr Blood Cancer* 61:120-127.

Neuwelt AJ, Wu YJ, Knap N, Losin M, Neuwelt EA, Pagel MA, Warmann S, Fuchs J, Czauderna P and Wozniak M (2009) Using acetaminophen's toxicity mechanism to enhance cisplatin efficacy in hepatocarcinoma and hepatoblastoma cell lines. *Neoplasia* 11:1003-1011.

Ohashi N and Kohno T (2020) Analgesic Effect of Acetaminophen: A Review of Known and Novel Mechanisms of Action. *Front Pharmacol* 11:580289.

Owumi SE, Andrus JP, Herzenberg LA and Herzenberg LA (2015) Co-administration of N-Acetylcysteine and Acetaminophen Efficiently Blocks Acetaminophen Toxicity. *Drug Dev Res* 76:251-258.

Pingali P, Wu YJ, Boothello R, Sharon C, Li H, Sistla S, Sankaranarayanan NV, Desai UR, Le AT, Doebele RC, Muldoon LL, Patel BB and Neuwelt A (2021) High dose acetaminophen inhibits STAT3 and has free radical independent anti-cancer stem cell activity. *Neoplasia* 23:348-359.

Pourbagher-Shahri AM, Schimmel J, Shirazi FM, Nakhaee S and Mehrpour O (2022) Use of fomepizole (4-methylpyrazole) for acetaminophen poisoning: A scoping review. *Toxicol Lett* 355:47-61.

Rasamison R, Besson H, Berleur MP, Schicchi A, Mégarbane B (2020) Analysis of fomepizole safety based on a 16-year post-marketing experience in France. *Clin Toxicol (Phila)* 58:742-747.

Saito C, Zwingmann C and Jaeschke H (2010) Novel mechanisms of protection against acetaminophen hepatotoxicity in mice by glutathione and N-acetylcysteine. *Hepatology* 51:246-254.

Thomsen MS, Loft S, Roberts DW and Poulsen HE (1995) Cytochrome P4502E1 inhibition by propylene glycol prevents acetaminophen (paracetamol) hepatotoxicity in mice without cytochrome P4501A2 inhibition. *Pharmacol Toxicol* 76:395-399.

Villarino AV, Kanno Y, Ferdinand JR and O'Shea JJ (2015) Mechanisms of Jak/STAT signaling in immunity and disease. *J Immunol* 194:21-27.

Wang Y, Pandak WM, Lesnefsky EJ, Hylemon PB and Ren S (2021) 25-Hydroxycholesterol 3-Sulfate Recovers Acetaminophen Induced Acute Liver Injury via Stabilizing Mitochondria in Mouse Models. *Cells* 10.

Wu YJ, Neuwelt AJ, Muldoon LL and Neuwelt EA (2013) Acetaminophen enhances cisplatin- and paclitaxel-mediated cytotoxicity to SKOV3 human ovarian carcinoma. *Anticancer Res* 33:2391-2400.

Xiao H, Guo Y, Li B, Li X, Wang Y, Han S, Cheng D and Shuai X (2020) M2-Like Tumor-Associated Macrophage-Targeted Codelivery of STAT6 Inhibitor and IKKbeta siRNA Induces M2-to-M1 Repolarization for Cancer Immunotherapy with Low Immune Side Effects. *ACS Cent Sci* 6:1208-1222.

Zhou H, Gurley EC, Jarujaron S, Ding H, Fang Y, Xu Z, Pandak WM, Jr. and Hylemon PB (2006) HIV protease inhibitors activate the unfolded protein response and disrupt lipid metabolism in primary hepatocytes. *Am J Physiol Gastrointest Liver Physiol* 291:G1071-1080.

JPET Fast Forward. Published on November 2, 2023 as DOI: 10.1124/jpet.123.001772
This article has not been copyedited and formatted. The final version may differ from this version.

Footnotes

Services and products in support of the research project were generated by the Virginia Commonwealth University Flow Cytometry, Cancer Mouse Models, and Microscopy Shared Resource, supported, in part, with funding from NIH-NCI Cancer Center Support Grant P30 CA016059 and the Analytical Core at KUMC supported in part by National Institute of General Medicine (NIGMS)-funded Liver Disease COBRE grant P30 GM118247. The work was supported by Swim Across America grant; VA grant 5IK2BX004914-02 to AN; and VCU Internal Medicine Seed Grant.

Department of Veterans Affairs (authors AN and AB) has a patent pending for concurrent use of CYP2E1 inhibitors and acetaminophen.

JPET Fast Forward. Published on November 2, 2023 as DOI: 10.1124/jpet.123.001772
This article has not been copyedited and formatted. The final version may differ from this version.

Legends for Figures

Figure 1. Fomepizole protects against AAP hepatotoxicity. A-C) BALB/c mice were treated as indicated and sacrificed the following day when they were weighed and serum analyzed. AAP concentrations in mg/kg. Used NAC 100 mg/kg and fomepizole 30 mg/kg unless otherwise indicated. D) Histology of liver analyzed 24 hours treatment as indicated. Scale bars are 0.5 mm (low magnification) and 0.05 mm (high magnification).Fomepizole and NAC concentrations were same as above. E) Serum AAP concentrations determined by ELISA at indicated time after treatment. AAP treatment concentrations in mg/kg. * < 0.05. Error bars represent SD.

Figure 2. NAC and fomepizole don't reverse AAP cytotoxicity against tumor cells in vitro. A) Protein Atlas was used to assess CYP2E1 RNA levels in various organs. LLC cells were cultured for 48 hours in AAP (1 mM), NAC (0.3 mg/mL) and or fomepizole (300 μM) and then analyzed via CCK8 assay (B) or LDH release assay (C). D) CCK8 experiment was repeated in 4T1 cells. AAP concentration 3 mM; fomepizole and NAC concentrations were same as above. E) CYP2E1 expression as assessed by RNA qPCR in the liver and tumor of a 4T1 tumor bearing mouse. Normalized for GAPDH levels. Error bars represent SD. * $p < 0.05$.

Figure 3. Fomepizole prevents free radical mediated AAP hepatotoxicity. A) Isolated hepatocytes from mice were treated with AAP (5 mM) and or fomepizole (1 mM) for 6 hours and analyzed using live cell imaging via fluorescent microscopy. B) 4T1 tumor bearing mice were treated in vivo with 500 mg/kg AAP and/or fomepizole (30 mg/kg) and 6 hours later frozen sections made of tumor and liver. DCFH staining was used for free radical imaging. Optical magnification was 40x (oil objective). C) Serum from mice treated as in (B) was analyzed for ldh as a marker of hepatotoxicity. D, E) C57BL/6 mice were treated with AAP (500 mg/kg)

and/or fomepizole (30 mg/kg) and 6 hours later liver and tumor (LLC) was analyzed for protein adduct formation (D) and reduced and oxidized glutathione content (E). For experiments shown in D and E, n=4 mice used per condition. Error bars represent SD. * < 0.05

Figure 4. AAP has anti-cancer activity in vivo against 4T1 breast tumors. A) BALB/c mice were injected with 4T1 breast cancer cells orthotopically. Treatment was 2x/week once palpable tumors formed with Vehicle (NAC, 100 mg/kg and fomepizole, 30 mg/kg) and/or AAP (650 mg/kg). Tumor size was monitored and mice were weighed. n=5 mice per condition. B) Treatment was with Vehicle (NAC 100 mg/kg and propylene glycol, 10%) or AAP 500 mg/kg. 4T1 tumor size was monitored and mice were weighed. n=5 mice per condition. At time of sacrifice serum was analyzed for ALT and BUN (C) and liver histology assessed (D). Scale bars 0.5 mm (low magnification) and 0.05 mm (high magnification). Error bars represent SD. * $p < 0.05$.

Figure 5. AAP with fomepizole rescue has anti-tumor activity against LLC intra-tracheal orthotopic model. A) Mice were injected intra-tracheally with LLC cells and 5 days later (upon getting an IVIS signal) treatment was begun with Vehicle (fomepizole 30 mg/kg and NAC 100 mg/kg) or AAP (650 mg/kg) twice weekly and IVIS signal followed over time. B) Bioluminescence intensity (BLI) was quantitated. C) Body weight over time during experiment. D) Serial sections of lungs from mice 5 and 9 were obtained every 150 μM. H&E stains were evaluated for tumor. E) Representative H&E stain showing tumor in NAC/FOM treated mouse and no tumor in AAP/NAC/FOM treated mouse. Scale bars 0.5 mm (low magnification) and 0.05 mm (high magnification). Error bars represent SD, and * $p < 0.05$.

Figure 6. High dose AAP has anti-tumor activity in surgical orthotopic model with NAC/propylene glycol rescue and the effect appears at least in part immune mediated. A)

JPET Fast Forward. Published on November 2, 2023 as DOI: 10.1124/jpet.123.001772
This article has not been copyedited and formatted. The final version may differ from this version.

Schematic of surgical orthotopic model. Treatment was Vehicle (100 mg/kg NAC and 10% propylene glycol) or AAP (500 mg/kg). B) IVIS images at conclusion of study. C) Tumor size at time of animal sacrifice, n=4 for vehicle (1 mouse passed from disease burden), n=6 for AAP. D) Mouse body weight during study. E) Experiment was repeated in NSG immune-compromised mice and IVIS images are shown with quantification (F), n=5/condition. Error bars represent SD and $p < 0.05$.

Figure 1

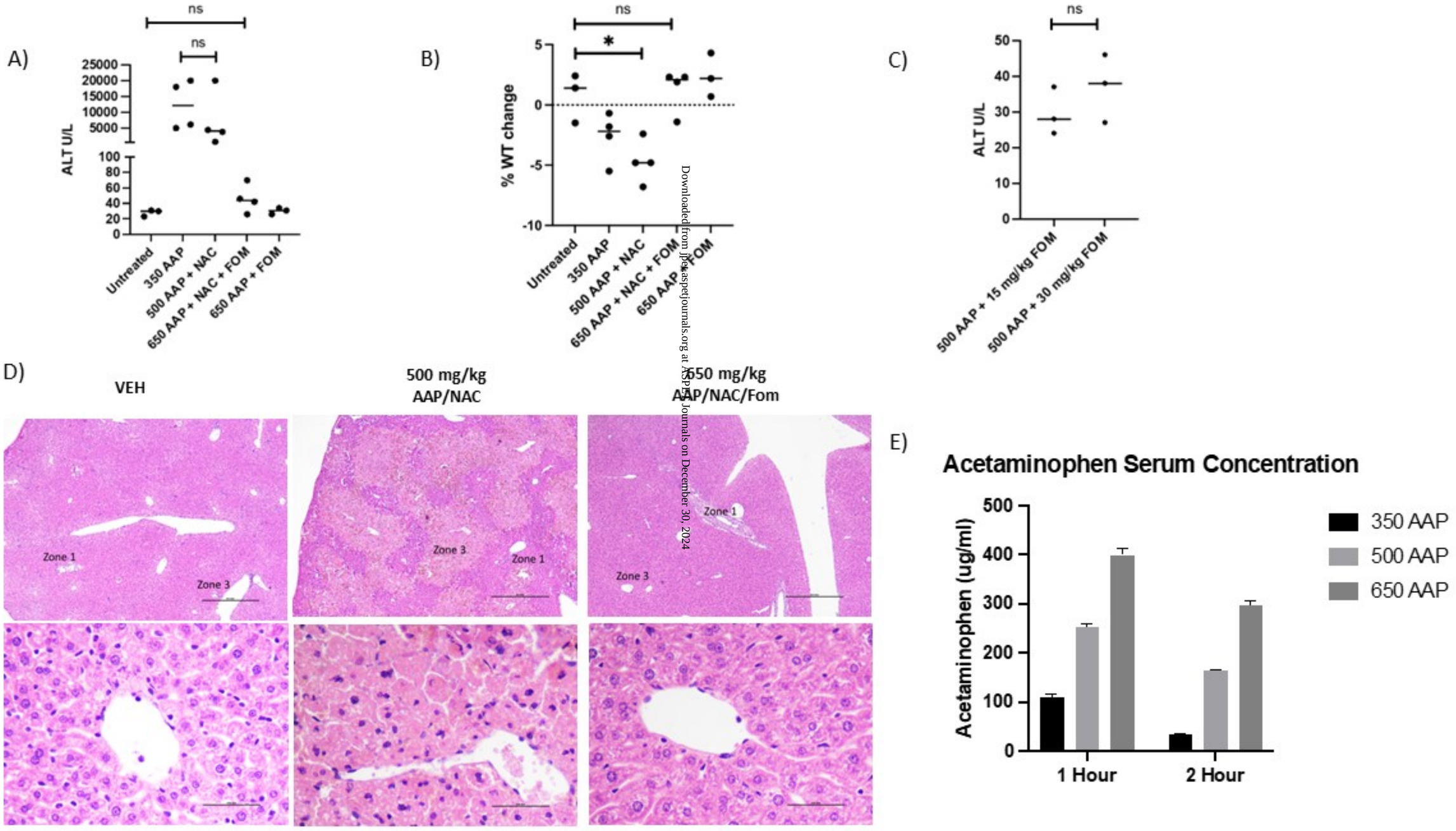

Figure 2

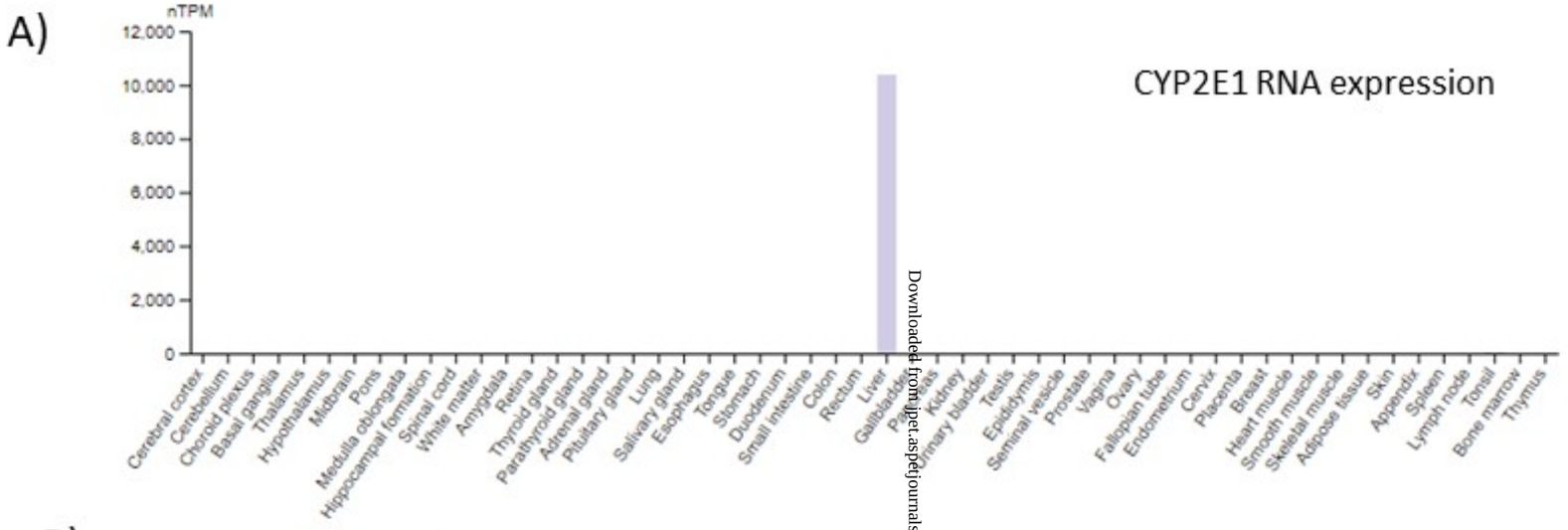

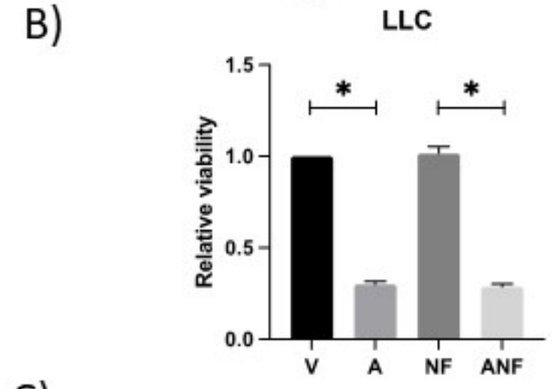

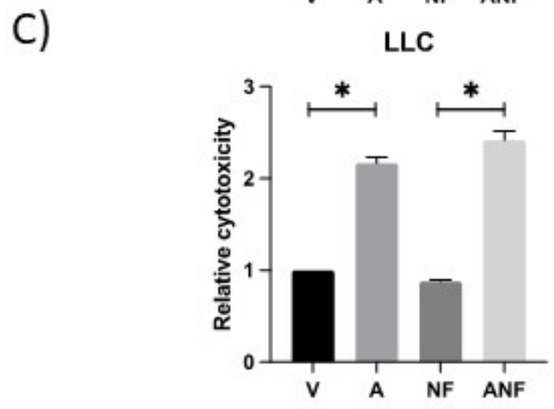

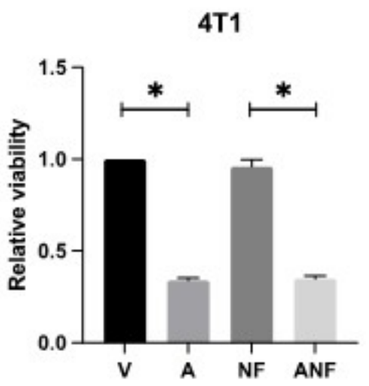

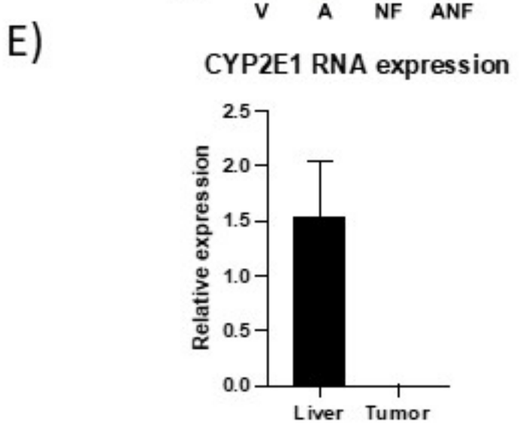

Figure 3

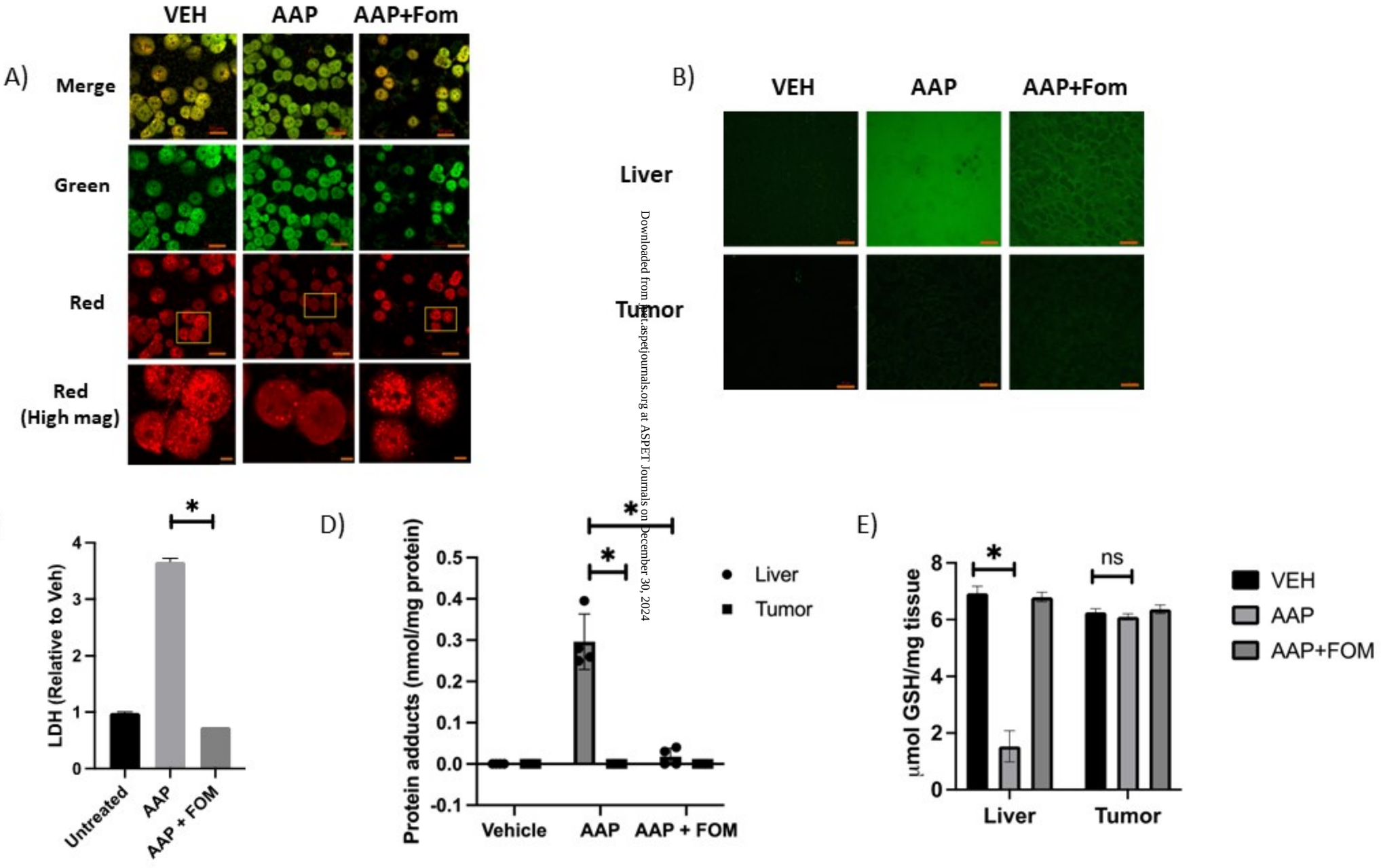

Figure 4

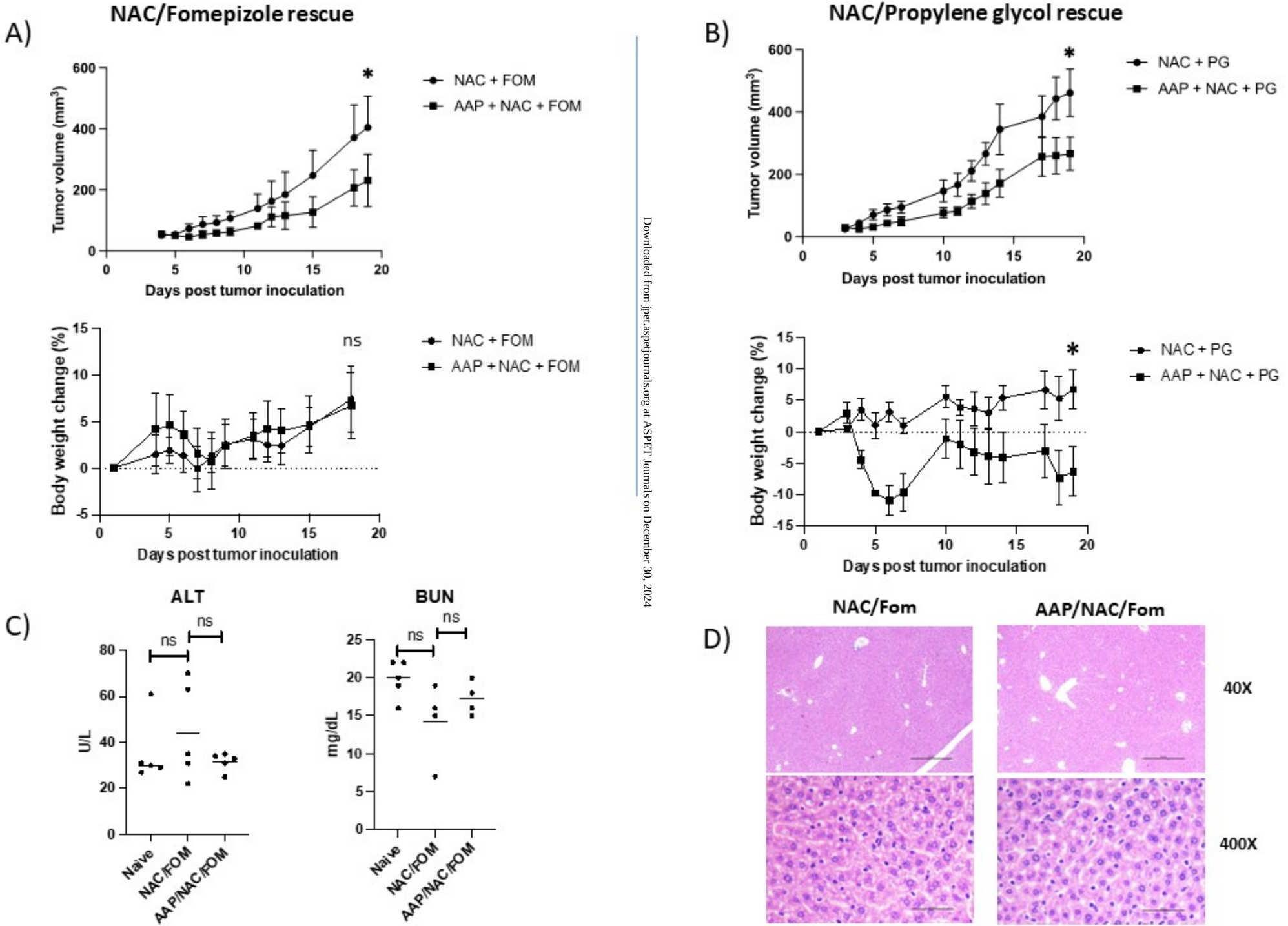

Figure 5

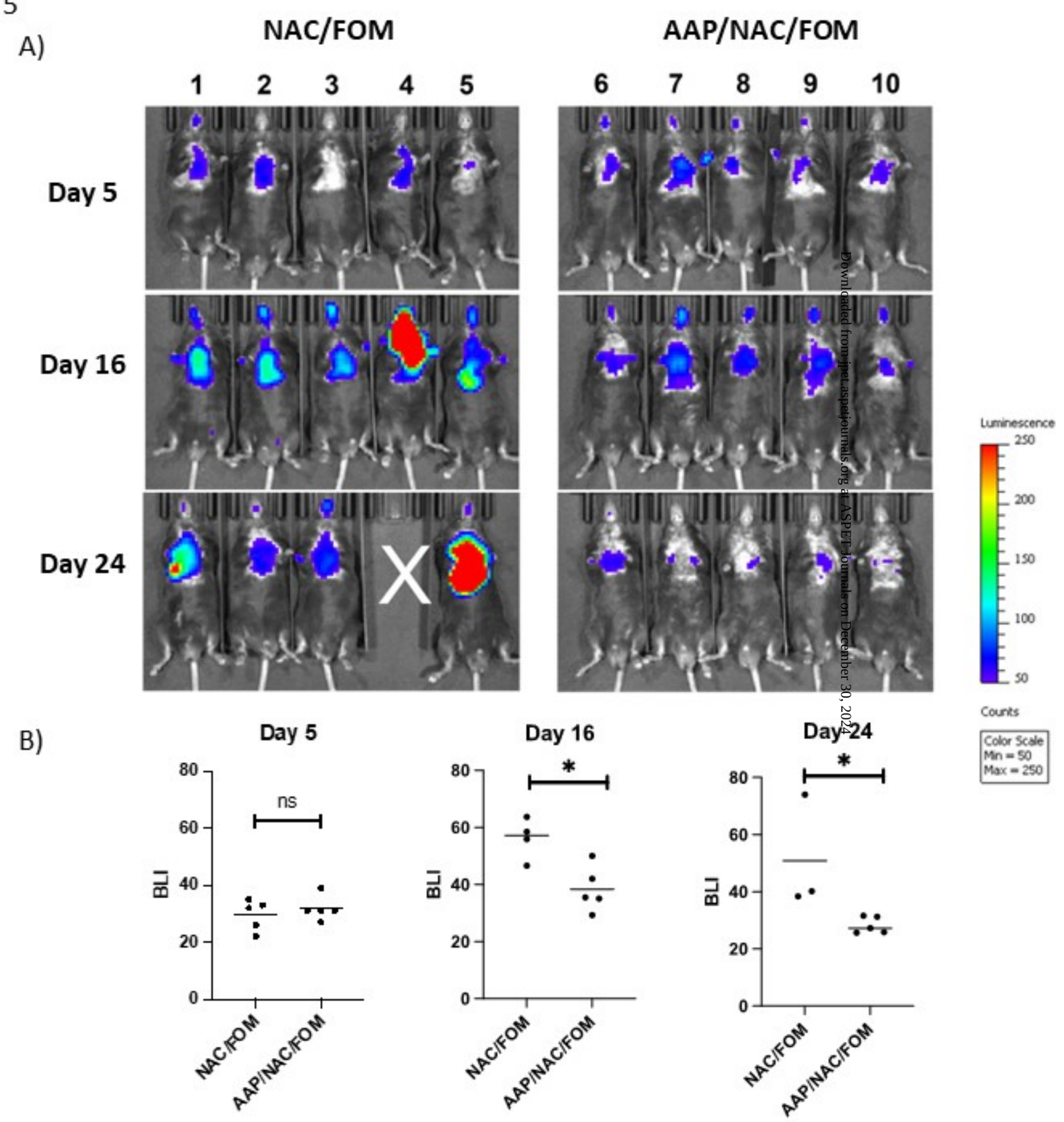

C)

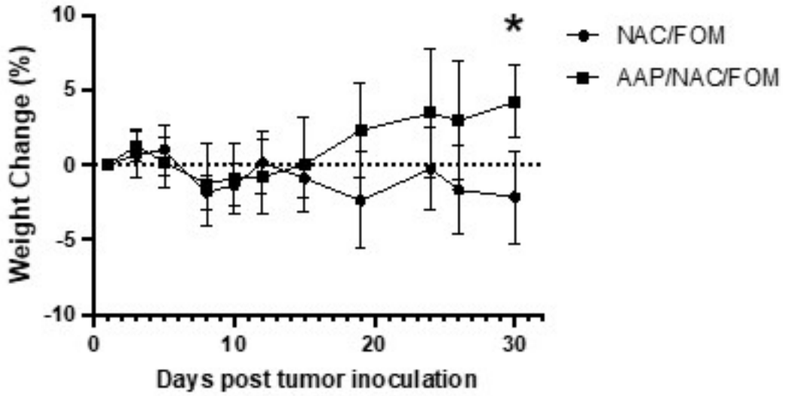

D)

Mouse	5	9
Treatment	NAC/ Fomepizole	AAP/NAC/ Fomepizole
Sections with tumor	9/9	0/9

E)

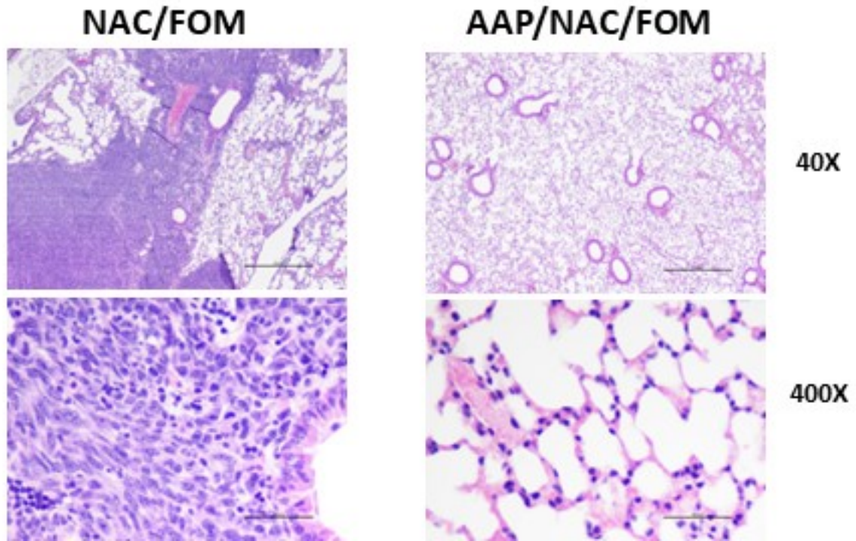

Figure 6